International Journal of Mechanical, Industrial and Aerospace Sciences
ISSN: 2517-9950
Vol:6, No:10, 2012

Autonomous Underwater Vehicle (AUV) Dynamics Modeling and Performance Evaluation

K. M. Tan, A. Anvar, and T.F. Lu

***Abstract*—**A sophisticated simulator provides a cost-effective measure to carry out preliminary mission testing and diagnostic while reducing potential failures for real life at sea trials. The presented simulation framework covers three key areas: AUV modeling, sensor modeling, and environment modeling. AUV modeling mainly covers the area of AUV dynamics. Sensor modeling deals with physics and mathematical models that govern each sensor installed onto the AUV. Environment model incorporates the hydrostatic, hydrodynamics, and ocean currents that will affect the AUV in a real-time mission. Based on this designed simulation framework, custom scenarios provided by the user can be modeled and its corresponding behaviors can be observed. This paper focuses on the accuracy of the simulated data from AUV model and environmental model derived from a developed AUV test-bed which was jointly upgraded by DSTO and the University of Adelaide. The main contribution of this paper is to experimentally verify the accuracy of the proposed simulation framework.

***Keywords*—**Autonomous Underwater Vehicle (AUV), simulator, framework, robotics, maritime robot, modeling.

I. Introduction

AUVS are untethered unmanned maritime robotic platforms which play a significant role in modern robotics. AUVs are involved in a number of maritime areas such as maritime security [9], oceanography [1] and submerged structure-inspection and maintenance. The main objective for this project is to develop a robust simulator capable of mimicking real-life AUV mission scenarios underwater. In order to achieve this, various knowledge of the physical aspects of the AUV such as the kinematics, dynamics, physical limitations, and environmental effects are required.

Compared to autonomous aerial or ground vehicle projects, underwater domain imposes the most restriction on sensory devices and its hardware [28].

Complicated and hazardous at-sea missions present many technical challenges to observe the AUV and also to diagnose the missions being carried out. Due to difficulties running a real-life test scenarios on the harsh ocean environment and resources limitations, the use of modeling and simulation for AUV development, trouble-shooting, and mission diagnostics are heavily justifiable [5][6].

One of the benefits of building a robust AUV simulator is that it provides a tool for further studies on AUV control systems. This is ideal for AUV control theory since it saves time and cost, where a designed control system can be observed and carried out using a simulated model rather than real-life mission testing. Models in this context represent the mathematical descriptions of the corresponding physical system of interest, while simulation represents the implementation in terms of hardware and software configurations. Both modeling and simulation are important to replicate the actual AUV system within the underwater environment.

Many research groups report different integration of thruster model, AUV model and environmental model. Although most commonly used dynamic model of AUV can be derived from the Newton-Euler equation of motion for a rigid body [8][15], the difference lies in quantification of the forces and lumped parameters of the equation of motion. In [15] the author reports a simulation framework which combines Newton-Euler equation of motion together with a robust controller to predict hydrodynamic parameters. The author reports successful implementation of the framework within simulated environment. Further literature review regarding the model specifics will be discussed in their respective sections.

The main focus of this paper is placed onto the theoretical analysis and the implementation of each model within the simulation framework and to display the integration of AUV model, and environmental model into the simulation framework and the accuracy of the simulation. This paper presents a generalized AUV 6DOF simulator framework and the accuracy of the proposed models.

The next section describes the background of the developed AUV. This is followed by an introduction to the hardware used. Section IV describes the physics, mathematical formulae and assumptions made in order to model a real-time AUV. The modeling criteria used in this project is based on a real world AUV developed by DSTO and The University of Adelaide, School of Mechanical Engineering. Section V describes the experimental procedures and the comparison between results real-life data and simulated data. The final section concludes this paper and presents future work for simulator upgrades.

II. System Overview

The whole simulation framework developed is based on an existing AUV test-bed [8], as shown in Fig. 1. The AUV system consists of four separate modules which can be seen along with their hardware in Table I.

K. M. Tan is a Graduate Engineer from the School of Mechanical Engineering, the University of Adelaide, South Australia, 5005 Australia.

A. Anvar is with the School of Mechanical Engineering, the University of Adelaide, South Australia, 5005 Australia (e-mail: amir.anvar@adelaide.edu.au).

T. F. Lu is with the School of Mechanical Engineering, the University of Adelaide, South Australia, 5005 Australia

TABLE I
AUV MODULES AND THEIR HARDWARE

Modules	*Hardware*
Inertial Navigation Sensors	Seabotic HPDC1500 Thrusters
	GPS receiver
	Compass
	ADXL Accelerometer
	Pressure sensor
	Doppler Velocity Log (DVL)
	Altimeter
Detection, Tracking and Identification Sensors	Sonar
	Stereo vision camera
Communication system	Radio Frequency (RF) air to air modems
	Underwater communication modems
Command and Control system	PC104 stack

Fig. 1 AUV Robot test bed

The structure of the simulation framework (Fig 2) shows the conversion of required trajectories to forces using inverse dynamics.

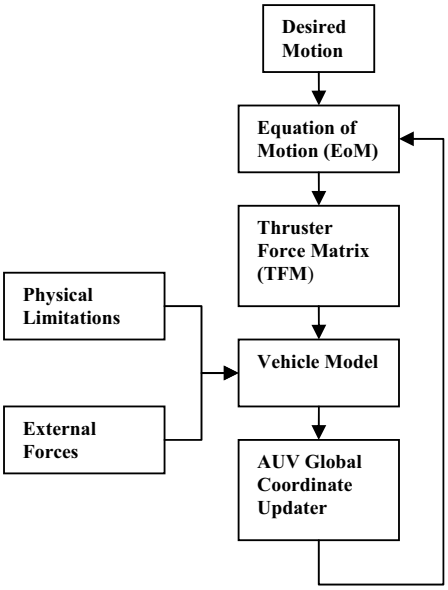

Fig. 2 AUV Simulation framework

III. MODELING

A. Model Assumptions

In the derivation of the equations that govern AUV model and Environmental Model, a few assumptions were made to simplify the complex equations, they are:

- AUV has constant mass and inertia tensor
- The formula takes account of axes not coinciding with the AUV's principal axis of inertia, therefore, the product of inertia is non-zero [13]
- AUV is designed to carry out missions in low-speed condition, hence the coupling terms can be reasonably neglected
- AUV is buoyant while carrying out its mission
- Mission is carried out in a shallow water environment

B. AUV Model

The AUV dynamic model is formulated using both a body fixed frame and a global frame. The body fixed frame describes the AUV motions, both rotational and translational as $\dot{V} = \left[\dot{v}_x, \dot{v}_y, \dot{v}_z, \ddot{\theta}, \ddot{\phi}, \ddot{\kappa}\right]^T_{AUV}$, where $\dot{v}_x, \dot{v}_y$ and $\dot{v}_z$ represent the accelerations in x, y, and z- axis while $\ddot{\theta}, \ddot{\phi}$ and $\ddot{\kappa}$ are the angular acceleration along x, y, and z-axis, as shown in Fig. 3.

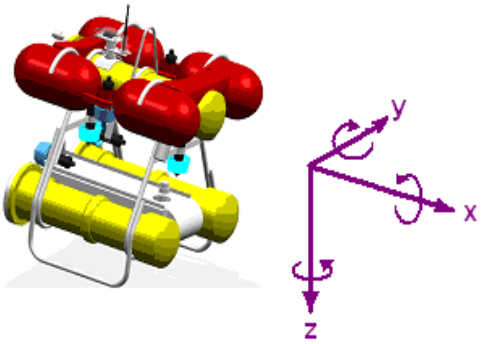

Fig. 3 AUV local frame

The proposed simulated and real life model uses 6 thrusters configuration as shown in Fig. 4 and Fig. 5. This configuration enables linear and rotational movements along x, y and z-axis.

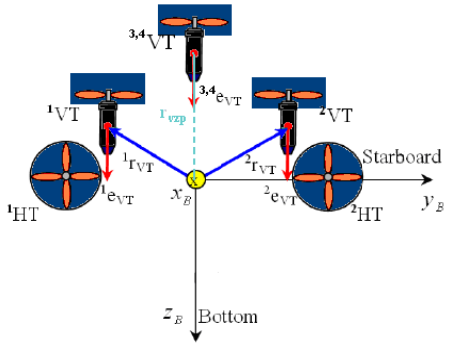

Fig. 4 Rear View of AUV with 6 Thrusters configuration

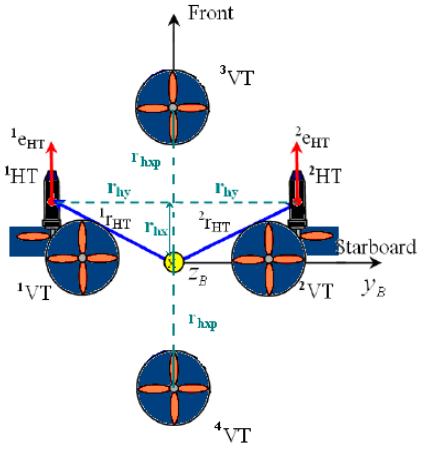

Fig. 5 Top View of AUV with 6 Thrusters configuration

The summary forces and torques generated is shown in Table II, where subscript x, y and z represents the forces and torques along x, y and z-axes. Table III and Table IV shows the measured position and orientation parameters of the developed AUV model which will be used within the simulator.

TABLE II
SUMMARY OF FORCES AND TORQUES GENERATED BY THRUSTERS

Forces, f_{TH}	f_x	$T_{HT_1} + T_{HT_2}$
	f_y	0
	f_z	$T_{VT_1} + T_{VT_2} + T_{VT_3} + T_{VT_4}$
Torques, τ_{TH}	τ_x (Roll)	$-r_{vy}T_{VT_1} + r_{vy}T_{VT_2}$
	τ_y (Pitch)	$-r_{hxp}T_{VT_3} + r_{hxp}T_{VT_4}$
	τ_z (Yaw)	$r_{hy}T_{HT_1} - r_{hy}T_{HT_2}$

TABLE III
POSITION VECTORS FOR THRUSTER CONFIGURATION

HORIZONTAL THRUSTERS	r_{HT_1}	$[r_{hx} \quad -r_{hy} \quad 0]^T$
	r_{HT2}	$[r_{hx} \quad r_{hy} \quad 0]^T$
VERTICAL THRUSTERS	r_{VT1}	$[0 \quad -r_{vy} \quad r_{vz}]^T$
	r_{VT2}	$[0 \quad r_{vy} \quad -r_{vz}]^T$
	r_{VT3}	$[r_{hxp} \quad 0 \quad -r_{vzp}]^T$
	r_{VT4}	$[-r_{hxp} \quad 0 \quad -r_{vzp}]^T$

TABLE IV
ORIENTATION VECTORS FOR THRUSTER CONFIGURATION

Horizontal Thrusters		*Vertical Thrusters*		***Vertical (Pitch) Thrusters***	
e_{HT1}	e_{HT2}	e_{VT1}	e_{VT2}	e_{VT3}	e_{VT4}
$\begin{bmatrix}1\\0\\0\end{bmatrix}$	$\begin{bmatrix}1\\0\\0\end{bmatrix}$	$\begin{bmatrix}0\\0\\1\end{bmatrix}$	$\begin{bmatrix}0\\0\\1\end{bmatrix}$	$\begin{bmatrix}0\\0\\1\end{bmatrix}$	$\begin{bmatrix}0\\0\\1\end{bmatrix}$

The motion of the AUV is comprised of both the translational and rotational components. Using Newton's second law of motion, the translational component can be the motion of the AUV is comprised of both the translational and rotational components. Using Newton's second law of motion, the translational component can be derived by considering the location of a body-fixed frame located at the AUV's centre of mass. As for the rotational component, the formula was derived based on total applied moments about the AUV's centre of mass. The final form of the AUV equation of motion can be simplified as seen in (1):

$$M_{RB}\dot{V} + C_{RB}(x)V = f_{total} \quad (1)$$

$$M_{RB}\begin{bmatrix}\dot{v}_x\\ \dot{v}_y\\ \dot{v}_z\\ \ddot{\theta}\\ \ddot{\phi}\\ \ddot{\kappa}\end{bmatrix} + C_{RB}(x)\begin{bmatrix}v_x\\ v_y\\ v_z\\ \dot{\theta}\\ \dot{\phi}\\ \dot{\kappa}\end{bmatrix} = \begin{bmatrix}f_x\\ f_y\\ f_z\\ \tau_x\\ \tau_y\\ \tau_z\end{bmatrix} \quad (2)$$

$$M_{RB}=\begin{bmatrix} m & 0 & 0 & 0 & mz_{CoG} & -my_{CoG}\\ 0 & m & 0 & -mz_{CoG} & 0 & mx_{CoG}\\ 0 & 0 & m & my_{CoG} & -mx_{CoG} & 0\\ 0 & -mz_{CoG} & my_{CoG} & I_{xx} & I_{xy} & I_{xz}\\ mz_{CoG} & 0 & -mx_{CoG} & I_{xy} & I_{yy} & I_{yz}\\ -my_{CoG} & mx_{CoG} & 0 & I_{xz} & I_{yz} & I_{zz}\end{bmatrix} \quad (3)$$

$$C_{RB}(x)=\begin{bmatrix} 0 & -m\dot{\kappa} & m\dot{\phi} & m\left(y_{CoG}\dot{\phi}+z_{CoG}\dot{\kappa}\right) & -mx_{CoG}\dot{\phi} & -mx_{CoG}\dot{\kappa}\\ m\dot{\kappa} & 0 & -m\dot{\theta} & -my_{CoG}\dot{\theta} & m\left(z_{CoG}\dot{\kappa}+x_{CoG}\dot{\theta}\right) & -my_{CoG}\dot{\kappa}\\ -m\dot{\phi} & m\dot{\theta} & 0 & -mz_{CoG}\dot{\theta} & -mz_{CoG}\dot{\phi} & m\left(x_{CoG}\dot{\theta}+y_{CoG}\dot{\phi}\right)\\ -m\left(y_{CoG}\dot{\phi}+z_{CoG}\dot{\kappa}\right) & my_{CoG}\dot{\theta} & mz_{CoG}\dot{\theta} & 0 & -I_{yz}\dot{\phi}-I_{xz}\dot{\theta}+I_{zz}\dot{\kappa} & I_{yz}\dot{\kappa}+I_{xy}\dot{\theta}-I_{yy}\dot{\phi}\\ mx_{CoG}\dot{\phi} & -m\left(z_{CoG}\dot{\kappa}+x_{CoG}\dot{\theta}\right) & mz_{CoG}\dot{\phi} & I_{yz}\dot{\phi}+I_{xz}\dot{\theta}-I_{zz}\dot{\kappa} & 0 & -I_{xz}\dot{\kappa}-I_{xy}\dot{\phi}+I_{xx}\dot{\theta}\\ mx_{CoG}\dot{\kappa} & my_{CoG}\dot{\kappa} & -m\left(x_{CoG}\dot{\theta}+y_{CoG}\dot{\phi}\right) & -I_{yz}\dot{\kappa}-I_{xz}\dot{\theta}+I_{yy}\dot{\phi} & I_{xz}\dot{\kappa}+I_{xy}\dot{\phi}-I_{xx}\dot{\theta} & 0\end{bmatrix} \quad (4)$$

M_{RB} represents the rigid body mass matrix and $C_{RB}(x)$ represents the state dependent matrix containing the rigid body coriolis and centrifugal terms. The right hand side of (1) is the vector sum of forces induced by AUV thrust forces and also the external environmental forces and moments. These external forces and moments are composed of hydrostatic and hydrodynamic forces acting onto the AUV.

C. Environmental Forces

An AUV will encounter various environmental forces when running missions underwater. These environmental forces can be classified into six different forms: buoyancy, added mass effect, potential damping, Froude-Kriloff, viscous damping, and lift. However, in this paper, only the effect of added mass and viscous damping will be considered. This is due to the nature of the experiments carried out, as well as most forces are small and negligible. In theory, the derivation of these hydrodynamic parameters is costly and practically impossible.

Conventional hydrodynamic parameter derivation methods involve towing tank trials of the vehicle itself [18], or scaled model free decay [30]. These methods provides complete model identification, however they are often time consuming and costly. As a consequence, cheaper and more robust method using onboard sensors are preferred. There are generally two commonly used hydrodynamic parameter identifications methods based on the usage of onboard sensors. One of them relies on offline parameter identification, as seen in [19][27][24]. While another one relies on online adaptive parameter identification [20][29]. In [4] the authors compared both on-line adaptive identification technique and off-line least-square method using experimental data obtained with John Hopkins University Remotely Operated Vehicle (JHUROV). The authors reported that the identification of hydrodynamic parameters can be obtained successfully using both online and offline techniques on decoupled, single degree of freedom dynamical plant models. In [24] the authors report the successful usage of offline weighted least square parameter identification on a decoupled plant. The authors report that the simulated plant velocity agrees with the

observed experimental velocity. In [8] the authors report the identification of a decoupled plant model of AUV in x-direction using ordinary least square method. The authors report the inaccuracy of data obtained from acceleration measurement and vehicle model which leads to large mean square error between the simulated forces and measured forces.

This proposed method is advantages for a real time simulation purpose, computational speed is required; hence no CFD software is integrated within the simulation protocol. One can derive the added mass of an object by considering the hydrodynamic force acting on it as it accelerates. By integrating the pressure over the area projected in the x-direction, the force caused by added-mass can be calculated.

$$F_{AMx} = \int_0^{\pi}\left[-\rho\left[\frac{\partial\phi}{\partial t}+\frac{1}{2}|\nabla\phi|^2\right]\right]\cos\theta 2\pi R^2\sin\theta d\theta = -\frac{2}{3}\rho\pi R^3 a_x \quad (5)$$

In this paper, the ordinary least square method is used as it provides a cost effective and relatively realistic evaluation of drag coefficients based on the dynamic model of the AUV. The underlying concept used consists of measuring the linear acceleration of the AUV in response to the applied thrust force, and applying a suitable numerical regression algorithm to obtain suitable hydrodynamic parameters:

$$M_{RB}\dot{V}+k_L V+k_Q V|V|-F_{TH}=\varepsilon, \quad (6)$$

where k_L and k_Q are linear and quadratic drag coefficients respectively, while ε accounts for the modeling errors.

A test is done by providing known thrust force, F_{TH} over a given discrete time interval, $[0,(n-1)T]$ to the AUV from rest. The resulting accelerations $\dot{V}=\dot{V}(t)$ are measured, and its corresponding velocities $V=V(t)$ can also be obtained through integration. With these data, k_L and k_Q can be acquired which minimize the mean square error (MSE)

$$MSE=\frac{1}{n}\sum_0^n \varepsilon^2(t). \quad (7)$$

The two basic requirements for implementing this method are to know the thruster outputs which provide known thrust forces, and to be able to measure the acceleration. Separate tests were conducted in a controlled environment to identify the thruster profile while the acceleration of the AUV is measured using the ADXL202 accelerometer. In the series of experiments carried out, data is collected from a series of input thrust forces over a time interval of 10s.

TABLE V
SUMMARY OF EXPERIMENTAL DATA COLLECTED FROM HYDRODYNAMICS PARAMETER VALIDATION BASED ON DIFFERENT THRUST FORCES

Experiment Set	*Input Thrust Forces (N) over the period of 10s*			k_L $\left(\frac{kg}{s}\right)$	k_Q $\left(\frac{kg}{m}\right)$	*MSE*
Set 1	5.61	12.24	18.86	18.57	72.24	8.24
Set 2	5.61	18.86	31.43	19.41	73.63	10.14
Average Term				18.99	72.94	

D.Simulation Framework

The simulated model is created based on the known thrust force profile and the understanding of AUV dynamics. The proposed simulation framework can be simplified as shown in Fig. 6.

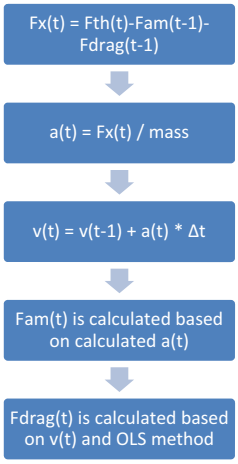

Fig. 6 Simulation process

The decoupled x-directional force at any instance, *Fx(t)* is calculated based on known thrust force at that instance subtracting projected environmental forces from previous time frame (in this case added mass effect, *Fam and* Drag Forces, *Fdrag*)

IV. HARDWARE

A. HPDC1500 Thruster

The AUV is equipped with three pairs of HPDC1500 thrusters from SeaBotix. These thrusters provide a maximum forward and backward thrust of 4.5kgf with blade speed running at 4500rpm.

Fig. 7 SeaBotix HPDC1500 thruster

B. Accelerometer

A dual axis ADXL202 accelerometer produced by Analogue Devices is integrated into the inertial navigation unit. This unit can measure accelerations with a full-scale range of ±2 *g* for low *g* and tilt applications. The sensitivity for each axis measurement is typically 15%/*g* when used in a water tank with surrounding water temperature of 22°C. ADXL202 is chosen because it has the ability to measure both AC accelerations (caused by vibrations) and also DC accelerations (inertial force and gravity) while producing an analogue output which can be directly measured by a microprocessor counter, without an analogue-to-digital converter.

Fig. 8 ADXL202 dual-axis accelerometer

C. Compass

An electronic magneto-inductive compass is installed on-board the AUV. This compass is used to accurately detect the AUV heading with an accuracy of up to ±0.1° when leveled. This electronic compass is properly calibrated with respect to the true north before conducting the experiments.

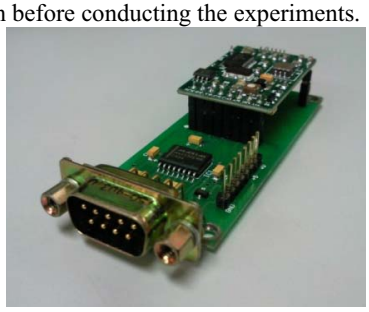

Fig. 9 Electronic compass

V. Experiment

In this section the experimental setup used for testing the accuracy of the models presented above is reported. The experimental setup consists of the AUV equipped with specified navigation system and a test-tank at DSTO.

Due to the nature of this experiment, the AUV is set to propel forward and backward progressively at seven different set speeds, with its corresponding thrust forces (see Table VI). Since the robot is symmetrical and remained buoyant, the roll, pitch and yaw movements caused by couplings are neglected.

TABLE VI
Thruster Speed Level and Corresponding Thrust Forces

Direction	*Speed Level*	Thrust Force (N)
Forward	+3	18.86
Forward	+2	12.24
Forward	+1	5.61
Stop	0	0
Backward	-1	-5.61
Backward	-2	-12.24
Backward	-3	-18.86

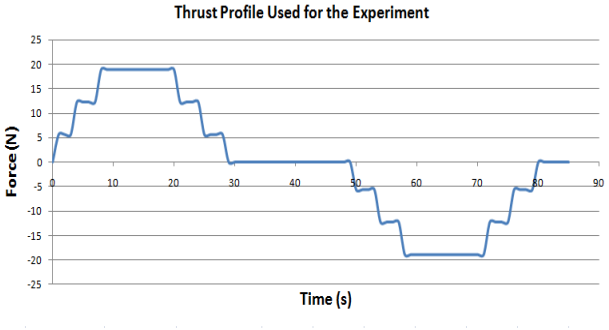

Fig. 10 Shows the thruster step command used in the experiment based on the tabulated thrust forces

The experiment is carried out in a test-tank located at the DSTO lab. The test-tank has a dimension of 7m x 5m x 6m (Length x Width x Depth) (see Fig 10). The AUV is set to navigate forward with progressive known thrust force from the two horizontal thrusters, halt, and then exert reverse thrust with the same speed in a reversed order. Fig. 11 shows the thruster force profile of the AUV moving in a stepped order.

A median filter for rejecting unwanted noise was applied to the acceleration data produced by the ADXL202. The median filter is configured to have length of 10 and width of 0.003m/s².

Fig. 11 Experimental trial within test tank

VI. Results and Discussions

In this section, the comparative results between the simulation and the real experiment are presented. First the result obtained from the ADXL202 accelerometer is extracted. Using these values, the corresponding forces and acceleration profile can be generated. Direct integration technique is applied to obtain velocity.

Based on the physical parameters of the AUV which can be computed using Table II and applying Equations 1, 2, 3 and 4, the simulated forces are acquired and used for comparison, see Fig. 12.

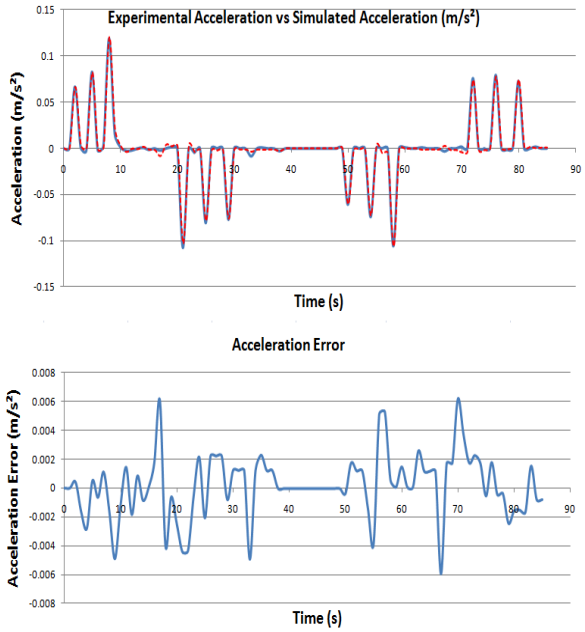

Fig. 12 Comparison of x-acceleration profile between experimental data and simulated data. First plot shows the numerical simulation acceleration and experimental acceleration versus time. Second plot shows the error between the two.

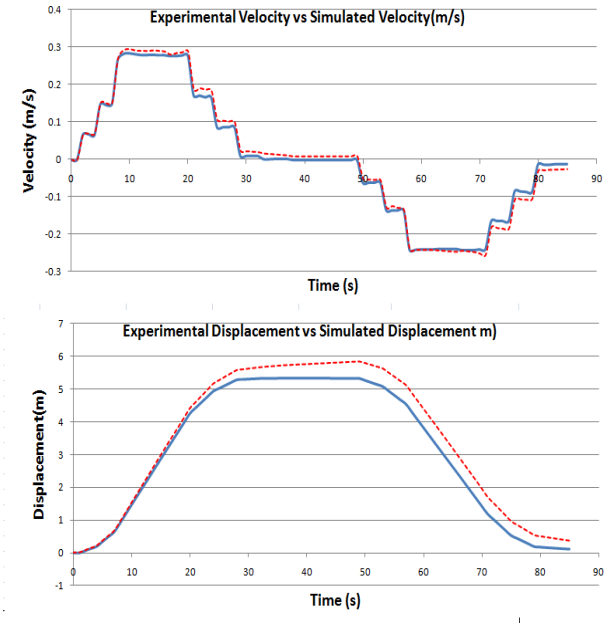

Fig. 13 Comparison of x-velocity and x-displacement profile between experimental data and simulated data. These graphs are obtained using direct integration method.

The experiments were conducted repetitively for eight times to minimise random errors caused by the accelerometer readings. Throughout the eight trials, five were validated and three were discarded due to external interferences which distorted the sensor readings. These external interferences mainly consist of uncleared buffer within the AUV thruster controller where both horizontal thrusters did not initiate forward thrust at the same time, causing much variation in the data. It is to be noted that, minimal control algorithms were used to maintain forward and backward thrust during the experiments. Among the 5 successful trials, no significant variations were observed. The difference between experimental data and the simulated forces is compared for each successful experimental trial. These force mean errors and absolute error are presented in Fig. 13. Experiment 1 has been chosen to compare graphically the results obtained with experimental data and the simulated data using direct integration techniques. The average standard deviation, σ is calculated to be 0.095.

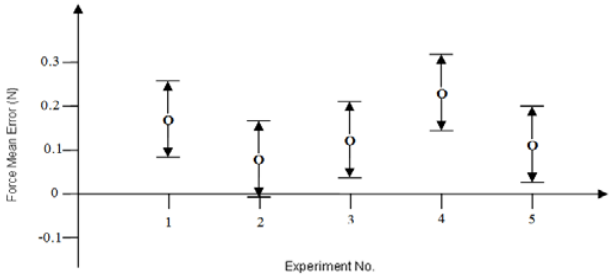

Fig. 14 Force Mean errors and standard deviations of five succesful trials

The performance of the proposed simulator is acceptable, as shown in Fig. 12, where the mean squared acceleration error 4.96254×10^{-6} m/s². Based on this model, further investigation where the speed of the AUV was increased and stability of the simulation were observed, as shown in Fig. 13. Since the test tank is of limited space, the acceleration of the AUV produced is limited to 0.6 m/s². According to the plot, the acceleration error showed in Fig. 13 increases as the acceleration of the AUV increases. From observation, this occurrence is due to the coupling effect of the AUV motion when high speed motion is being performed. Notice that, this is tested at an extreme case on a small water tank, and the conclusion made is based on both observation and numerical analysis.

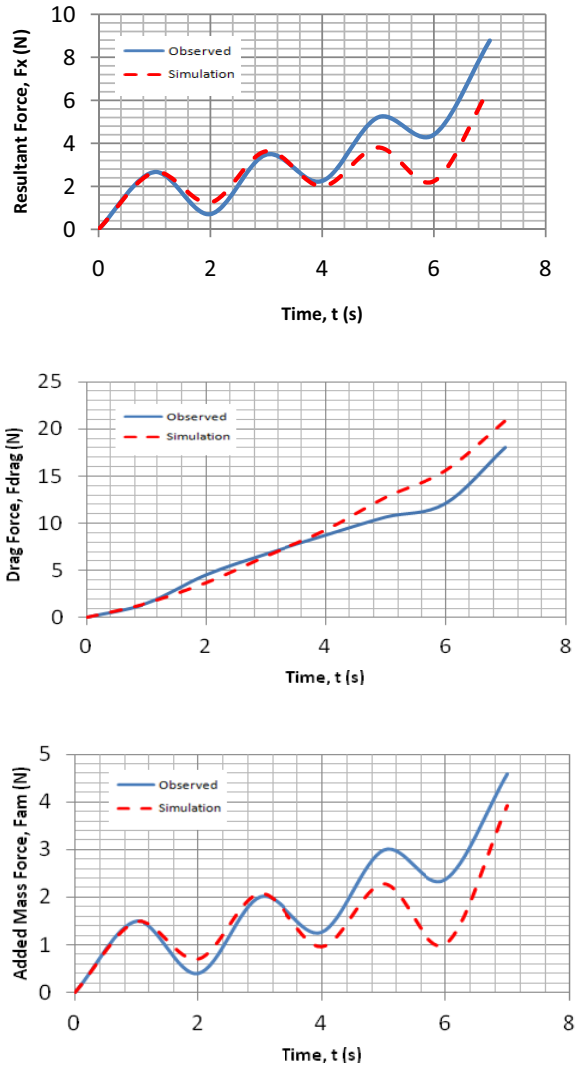

Fig. 15 Comparison of decoupled x-directional profile between observed experimental data and simulated data for acceleration exceeding 0.5m/s².

As expected, the simulated result is slightly more than the observed experimental outcome. This minor difference occurred due to the experimental assumption where the motion of the AUV can be modeled using decoupled dynamics. From observation, since the test tank is fairly small with solid surfaces, having the AUV move at higher speed will induce lift force causing the coupling effect to increase. It is to be noted that since the least-square method requires both velocity and acceleration, the better the signal obtained from the hardware, the closer the simulated data will get to the observed experimental data. It is to be emphasized that the experiments and observations were carried out based on low speed maneuvers and fixed pause rate to cope with the unaccounted environmental forces such as potential damping, lift, and Froude-Kriloff forces.

VII. Conclusion

This paper presented to the best of knowledge, a comparison between real-time scenario data and the simulated data using the proposed models. Decoupled, single degree of freedom dynamical plant models identified using combined AUV model and the environmental model were presented and evaluated. The comparison shows fairly accurate results for a simple navigation scenario. In order to simplify the verification process, common assumptions have been applied. The AUV is assumed to be buoyant and symmetrical at all times. The experiment has been conducted in an enclosed test-tank with the AUV running at low speed across the tank. Extensive uncoupled experiments were run to identify the thruster properties, sensor functionality and sensitivities. It has to be noted that single axis formula were used to simplify the environmental forces for comparison purposes.

For future work, the addition of heteroceptive sensors, such as a Doppler Velocity Log (DVL) will be installed. This will provide valuable real-time velocity data for more accurate measurements. Also, multiple scenarios which involve six degree of freedom navigation will be considered. The coupling effect caused by evaluating multiple degrees of freedom will also be investigated.

Acknowledgment

The authors would like to acknowledge the financial and in-kind support received from DSTO and The University of Adelaide, School of Mechanical Engineering. A special thanks to Graeme Coulter from DSTO for his invaluable knowledge regarding AUV hardware integration.

References

[1] B. Allen, R. Stokey, T. Austin, N. Forrester, R. Goldsborough, M. Purcell, C. von Alt, "REMUS: A small low cost AUV; System description, field trials, performance results," Proceedings of IEEE Ocean 97, pp. 994-1000, 1997.

[2] C. Payne, *Principles of Naval Weapon Systems*, 2006, Naval Institute Press, USA.

[3] C. Silvestre, A. Pascoal, and A.J. Healey, "AUV control under wave disturbances: An application of mixed design methods," Proceedings of CONTROLO '98 (3rd Portugese Conference on Automatic Control), Coimbra, Portugal, September 1998, pp 423-429.

[4] D.A. Smallwood, and L.L. Whitcomb, "Adaptive Identification of dynamically positioned underwater robotic vehicles,"*IEEE Trans.Control Systems Technology,* vol/ 11. no. 4, pp. 505-515, July 2003.

[5] D.P. Brutzman, Y. Kanayama, M.J. Zyda, "Autonomous Underwater Vehicle Technology,"*Proceedings of the 92' Symposium on Autonomous Underwater Vehicle Technology,* pp. 3-10, 1992.
[6] D.P. Brutzman, M.R. Macedonia, and M.J. Zyda, "Internetwork Infrastructure Requirements for Virtual Environments," *Proceedings of the VRML'95 Symposium*, pp. 95-104, 1995.
[7] E. Omerdic, "Thruster fault accomodation for underwater vehicles," *First IFAC workshop on guidance and control of underwater vehicles GCUV' 03,* Newport, South Wales, UK., April 2003 ,pp. 221–226.
[8] G. Conte, S. M. Zanoli, D. Scaradozzi, and A. Conti, "Evaluation of hydrodynamics parameters of a UUV. A preliminary study," *1st International Symposium on Control, Communications and Signal* Processing, pp. 545–548, 2004.
[9] G. Sten, P. E. Hagen, N. Størkersen, K. Vestgård and P. Kartvedt, "AUV based mine hunting demonstrated from MCMV," UDT Europe 2002, La Spezia, Italy, June 2002.
[10] H. Singh, "An entropic framework for AUV sensor modelling [Ph.D. Thesis]," 1995, Massachusetts Institute of Technology, 133 p.
[11] J.B. Lundberg, "Alternative algorithms for the GPS static positioning solution". *Applied Mathematics and Computation* (Elsevier), 2001, vol. 119 (1): pp21-34.
[12] J.J. Craig, Introduction to Robotics: Mechanics and Control*,* 3rd ed., New Jersey, 2005.
[13] J.N. Newman, *Marine Hydrodynamics.* Cambridge, MA: MIT Press, 1977.
[14] J.S. Riedel, "Seaway learning and motion compensation in shallow waters for small AUVs", 1999, PhD Thesis, NPS.
[15] J. Yuh, "Modelling and control of underwater robotics vehicles," *IEEE Trans. Syst., Man., Cybern.,* vol. 20, no. 6, pp. 1475-1483, 1990.
[16] K.M.Tan, T. Liddy, A. Anvar, and L. Tien-Fu, "The advancement of an autonomous underwater vehicle (AUV) Technology," *Proceedings of Industrial Electronics and Applications*, 2008, Singapore, pp336-341.
[17] K.M.Tan, A. Anvar, and L. Tien-Fu, "6 Degrees of Freedom (DOF) Maritime Robotic Simulation Framework," *11th International Conference on Control, Automation, Roboitics and Vision,*Singapore, December 2010.
[18] K.R. Goheen, "The modeling and control of remotely operated underwater vehicles," Ph.D. dissertation, University of London, 1986.
[19] K. Goheen, and E. Jeffreys, "The application alternative modeling techniques to ROV dynamics," *IEEE International Conference on Robotics and Automation,* pp. 1302-1309, 1990.
[20] K. Narendra, and A. Annaswamy. *Stable Adaptive Systems.* Prentice-Hall, NY, 1988
[21] L.E. Kinsler, A.R. Frey, A.B. Coppens, and J.V. Sanders, *Fundamentals of Acoustics*, 4th ed., Wiley, 2000, New York, pp448-450.
[22] L. Molnar, "A hybrid control architecture development for the guidance, navigation and control of the tethra prototype submersible vehicle," Ph.D. Thesis, University of Limerick, 2006.
[23] M.A. Ainslie, J.G. McColm, "A simplified formula for viscous and chemical absorption in sea water", Journal of the Acoustical Society of America, 1998, vol.103 (3), 1671-1672.
[24] M. Caccia, G. Indiveri, and G. Veruggio, "Modeling and Identification of Open-Frame Variable Configuration Unmanned Underwater Vehicles ," *IEEE J. Oceanic Eng.,* vol. 25, no. 2, pp. 227-240, April 2000
[25] P. Fofonoff, R. Millard, "Algorithms for computation of fundamental properties of seawater", 1983, UNESCO Technical Papers in Marine Science 44, UNESCO.
[26] R.J. Urick, Principles of Underwater Sound, 3rd ed., McGraw Hill, New York, 1983.
[27] S. Eiani-Cherif, G. Lebret, and M. Perrier, "Identification and control of a submarine vehicle," *Proceedings of the 5th IFAC Symposium on Robot Control,* pp.327-332, Nantes, France, 1997.
[28] S. Feijun, P.E. An, A. Folleco, "Modeling and simulation of autonomous underwater vehicles: design and implementation," *IEEE Jounal of Oceanic Eng.,* vol. 28, no. 2, pp. 283-296, April 2003.
[29] S. Sastry, and M. Bodson, *Adaptive Control: Stability, Convergence, and Robustness.* Prentice-Hall, 1989.
[30] Y.H. Eng, W.S. Lau, E. Low, G. Seet, and C.S. Chin, "Estimation of Hydrodynamics Coefficients of an ROV using Free Decay Pendulum Motion,"*Engineering Letters*, 2009.